Low-temperature Tolerant Lithium-rich Manganese-based Cathode Enabled by Facile SnO_2 Decoration

Diaohan Wang[1], Wenlei Wang[1], Kaihua Li[1], Jinze Song[1], Xinhai Yuan[1], Qinghong Huang[1], Zexun Tang[2]*, Lijun Fu[1]*, Yuping Wu[1]

[1]State Key Laboratory of Materials-Oriented Chemical Engineering, College of Energy Science and Engineering, and School of Chemistry and Molecular Engineering, Nanjing Tech University, Nanjing, 211816, Jiangsu Province, China

[2]College of Materials and Chemical Engineering, Hunan Institute of Engineering, Xiangtan, 411104, Hunan Province, China

Email Addresses: l.fu@njtech.edu.cn; lijunfufu@sina.com (L. F.); tangzexun@163.com (Z. T.)

Supporting Information

EXPERIMENTAL SECTION

Material Preparation

The pristine LLOS cathode material, denoted as $Li[Li_{0.144}Ni_{0.136}Co_{0.136}Mn_{0.544}]O_2$ or expressed as $0.336Li_2MnO_3 \cdot 0.664LiNi_{0.239}Co_{0.239}Mn_{0.451}O_2$, was synthesized employing the carbonate co-precipitation method. The raw materials of $MnSO_4 \cdot H_2O$, $NiSO_4 \cdot 6H_2O$, and $CoSO_4 \cdot 7H_2O$ with a molar ratio of 4:1:1. These compounds were dissolved in deionized water to formulate a 2.0 M solution of mixed metal ions (called mixed solution A). Concurrently, a 2.0 M $NaCO_3$ solution was prepared, herein denominated as mixed solution B.

The pH value of mixed solution (comprising mixed solutions A and B) was maintained at 7.5 by using aqueous ammonia. Subsequent to a 16-hour stirring period at a stable temperature of 55 ℃, a co-precipitated mixture denoted as $Ni_{0.1}Co_{0.1}Mn_{0.4}[CO_3]_{0.6}$ was formed. Next, the precipitated compound was subsequently filtered, washed, and subjected to drying at 80 ℃ for a duration of 12 hours. After that, the pretreated precursors were mixed with Li_2CO_3, with 5 wt.% excess. The mixed precursor was initially subjected to a heat treatment at 500 ℃ for 5 hours and subsequently calcined at 850 ℃ for 12 hours in an air atmosphere to get the pristine materials, designated as LLOS.

To modify the $Li[Li_{0.144}Ni_{0.136}Co_{0.136}Mn_{0.544}]O_2$ material with SnO_2, 10 mg of nano-SnO_2 and 1 g of LLOS were dispersed in 10 mL of isopropyl alcohol and subjected to ultrasonic agitation for one hour. The mixture was then continuously stirred at 80 ℃ until complete solvent evaporation. The resulting powder was heated under the temperature of 600 ℃ for 4 h in air and cooled to room temperature, getting the final S-LLOS sample.

Material Characterization

Crystalline structure of the samples was analyzed by X-ray diffraction with Cu Kα radiation and the samples were scanned from 2θ = 10-80° at a scan rate of 10° per minute. The morphologies of the materials were investigated via field-emission scanning electron microscopy (FESEM) (JSM-7800F, JEOL, Japan). The elemental contents of the samples were obtained *via* analysis on an Elementar Vario EL cube. X-ray photoelectron spectroscopy (XPS) was performed on a Kratos AXIS Ultra DLD. For the XPS test, the cell was disassembled in a glovebox, and the composite powder was collected after rinsing with dimethyl carbonate (DMC) and dried. To get deep insight into the enhanced cycle performance of the electrode after SnO_2 modification, half-cells were disassembled within an argon-filled glovebox and washed with dichloromethane (DMC) to obtain electrodes cycled for different cycles. The valence states of elements in LLOS and S-LLOS, were calibrated using a C 1s binding energy value of 284.8 eV.

Electrochemical measurement

Electrochemical performances of the samples were tested in CR2025 coin cells with galvanostatic cycling. The positive electrodes including active materials(80wt %), carbon black (10wt %), and polyvinylidene fluoride (10wt %) were added in N-methyl pyrrolidinone (NMP), and then the slurry was casted on Al foil. After drying at 80 °C for 12h, the electrodes were assembled into CR2025 coin cells in a glovebox filled with argon. The cells were composed of lithium metal as the anode, and Celgard 2400 membrane as the separator. The electrolyte was 1.0 M LiPF6 (Nanjing MJS Energy Technology Co., Ltd) dissolved in a mixture of ethylene carbonate/ethyl methyl carbonate (1:1, volume ratio). Based on the amount of separator and active material used, 50 μL electrolyte was added to each cell. CV plots were recorded on an electrochemical workstation (CHI660 Chenhua, Shanghai) and the scanning rate of cyclic voltammetry (CV) curves was 0.2 mV s^{-1} in the voltage range of 2.0-4.8 V. Galvanostatic charge/discharge tests were performed on a LAND Test System (LAND 2001 CT Wuhan China) at 25 °C. Nyquist plots were obtained with an AC oscillation amplitude of 5 mV in the frequency range of 100 kHz to 0.01 Hz at various

temperatures. The Galvanostatic intermittent titration technique (GITT) was employed by charging/discharging the cells for a duration of 10 minutes at a current density of 50 mA g^{-1}, based on the stabilized capacity, followed by a 40-minute relaxation period. Then diffusion coefficient (D_{Li^+}) from GITT was calculated by the following equation (Fick's second law). Where τ, m_B, M_B, V_M, and S denote the time duration of the current pulse, the mass, the molar mass, the molar volume of active materials, and the electrode area, respectively. ΔEs and ΔEt refer to the steady-state potential alteration caused by the current pulse and the potential variation during constant current, respectively.

$$D_{Li^+} = \frac{4}{\pi\tau}\left(\frac{m_B V_M}{M_B S}\right)^2\left(\frac{\Delta Es}{\Delta Et}\right)^2\left(\tau \ll \frac{L^2}{D_{Li^+}}\right)$$

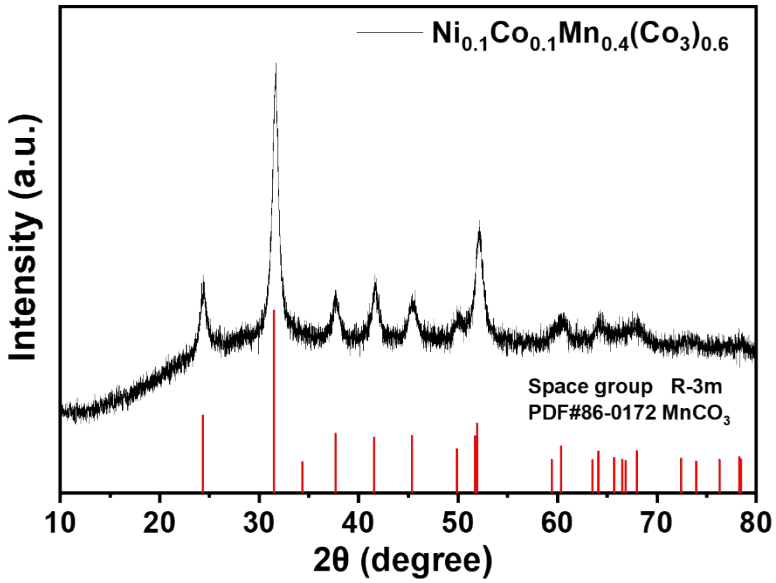

Figure S1. XRD patterns of the $Ni_{0.1}Co_{0.1}Mn_{0.4}[CO_3]_{0.6}$ precursor.

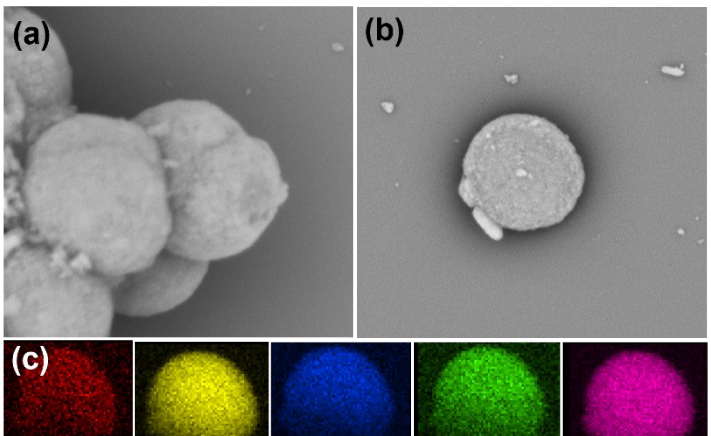

Figure S2. SEM and EDS images of the $Ni_{0.1}Co_{0.1}Mn_{0.4}[CO_3]_{0.6}$ precursor.

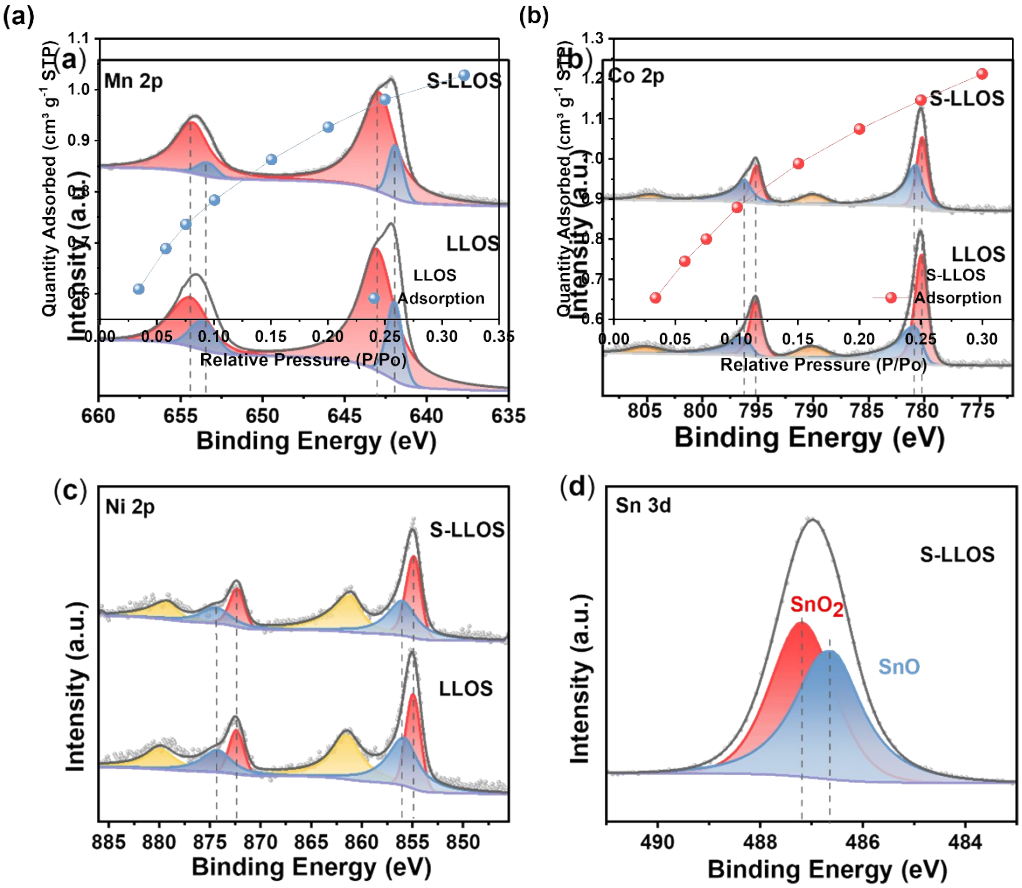

Figure S3. Nitrogen adsorption isotherms of LLOS and S-LLOS.

Figure S4. XPS analyses of LLOS and S-LLOS: (a) Mn 2p, (b) Co2p, (c) Ni 2p and (d) Sn 3d.

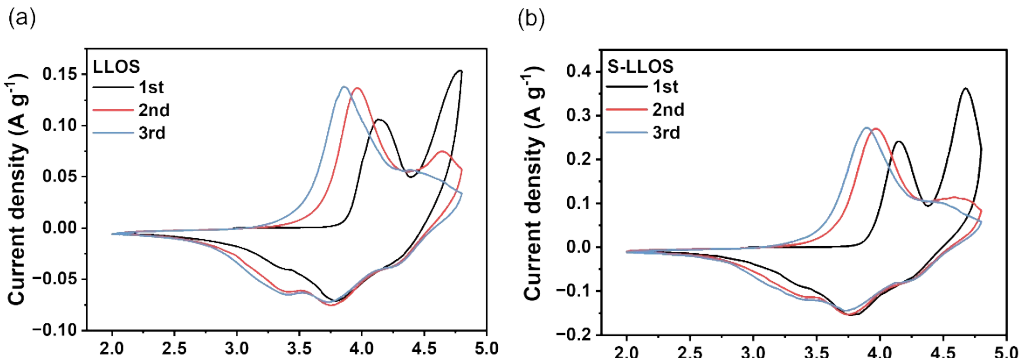

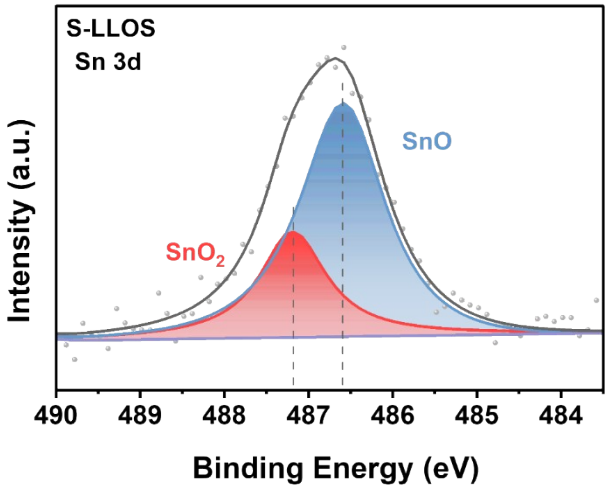

Figure S5. The CV curves of (a) LLOS and (b) S-LLOS during the first three cycles at a scan rate of 0.2 mV s^{-1} in the voltage range of 2.0−4.8 V at room temperature.

Figure S6. XPS spectrum of Sn 3d for S-LLOS sample after five cycles at room temperature.

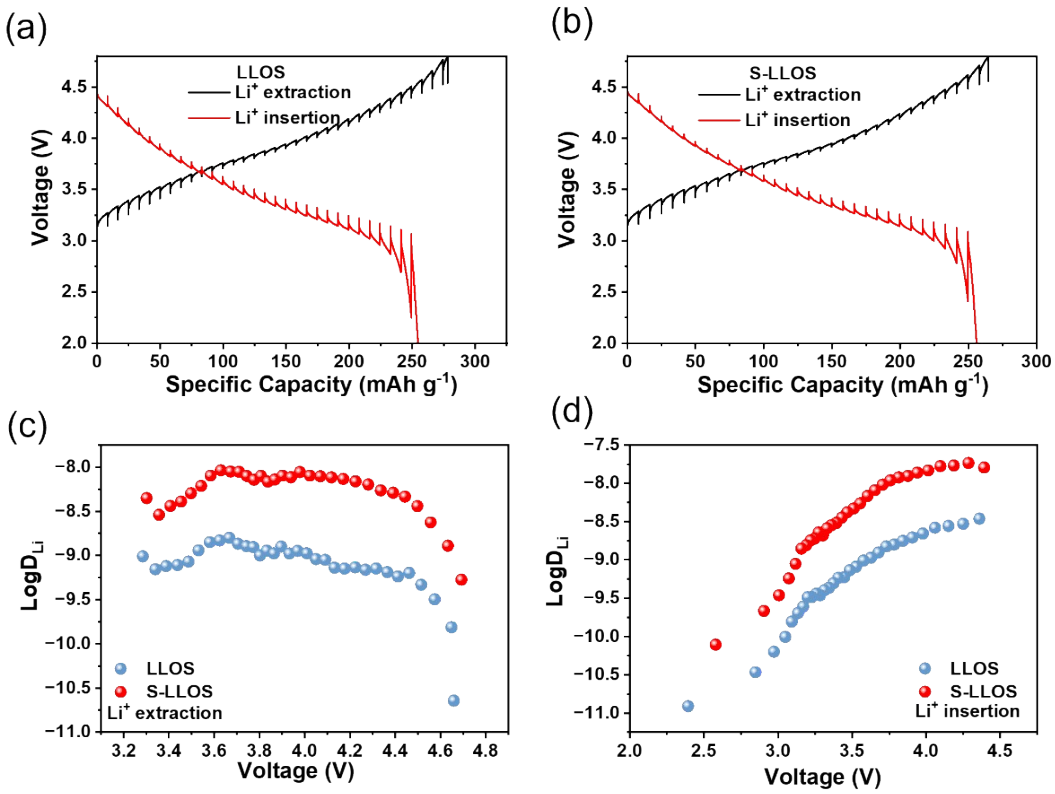

Figure S7. The GITT curves of (a) LLOS and (b) S-LLOS; (c, d) The calculated

Log D_{Li^+} values of two electrodes during charge and discharge processes.

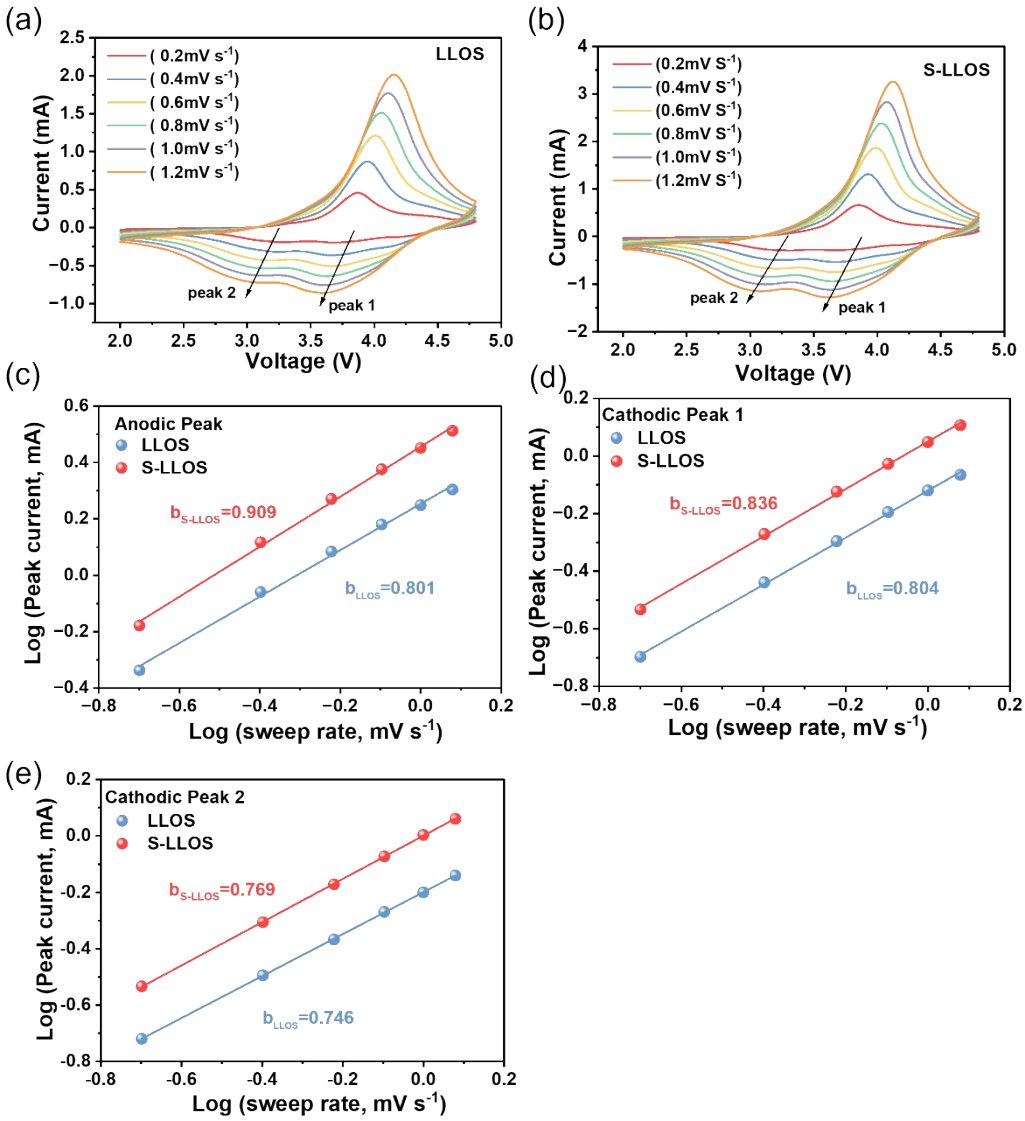

Figure S8. The CV curves at different scan rates for (a) LLOS and (b) S-LLOS. (c-e) the b values obtained via fitting according to log(i)=b log(v) + log(a).

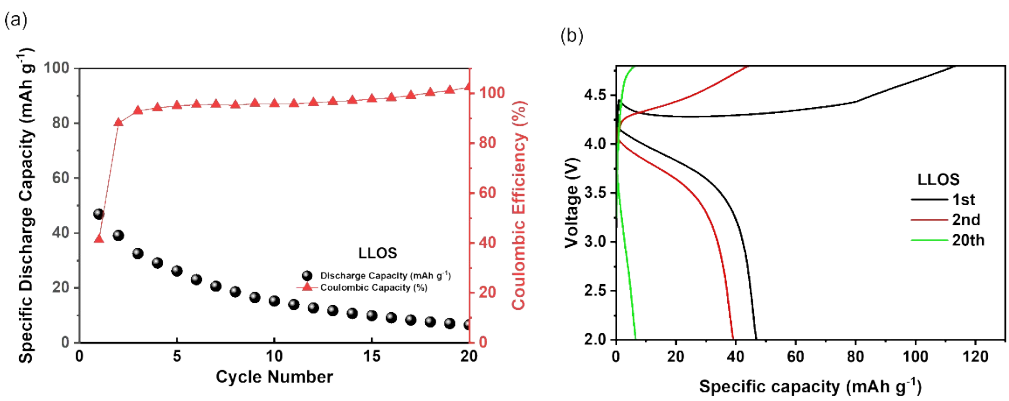

Figure S9. (a) The charge-discharge curves of (b) LLOS and (c) S-LLOS at -20 °C.

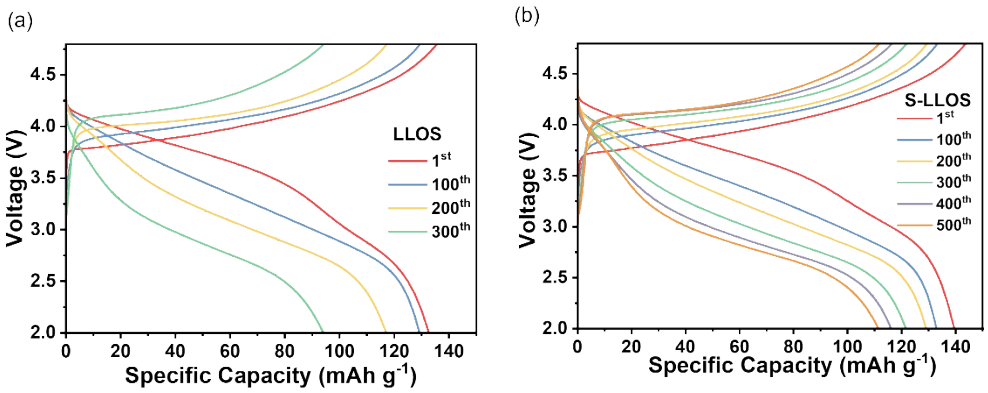

Figure S10. The charge-discharge curves of (a) LLOS and (b)S-LLOS at 0 °C after pre-cycled at room temperature for 5 times.

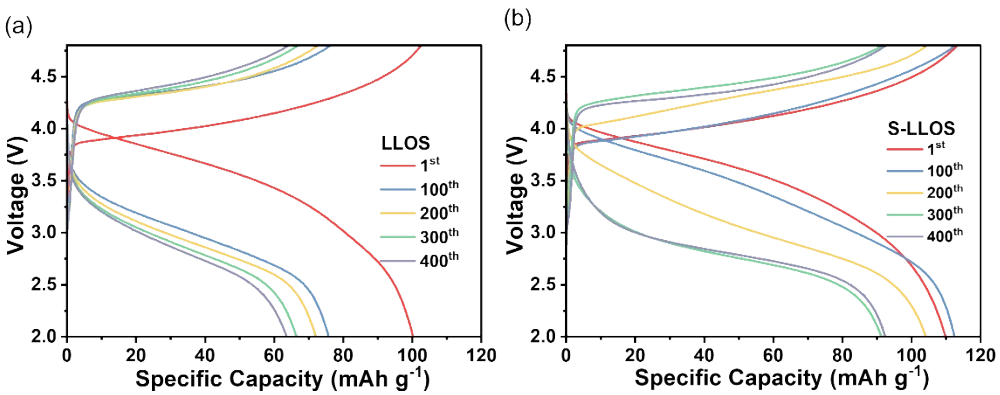

Figure S11. The charge-discharge curves of (a) LLOS and (b)S-LLOS of different cycle numbers at -20 °C after pre-cycled at room temperature for 5 times.

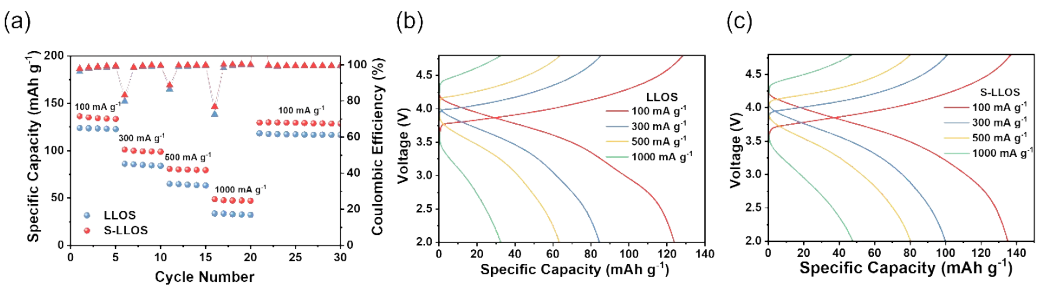

Figure S12. The rate performance for LLOS and S-LLOS at 0 °C (a). The charge/discharge curves of (b) LLOS and (c) S-LLOS at 0 °C at different rates.

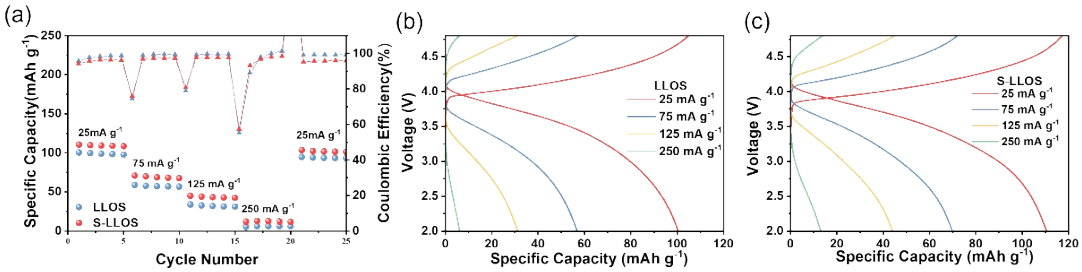

Figure S13. The rate performance for LLOS and S-LLOS at -20 °C. (a) The charge/discharge curves of (b) LLOS and (c) S-LLOS at different rates.

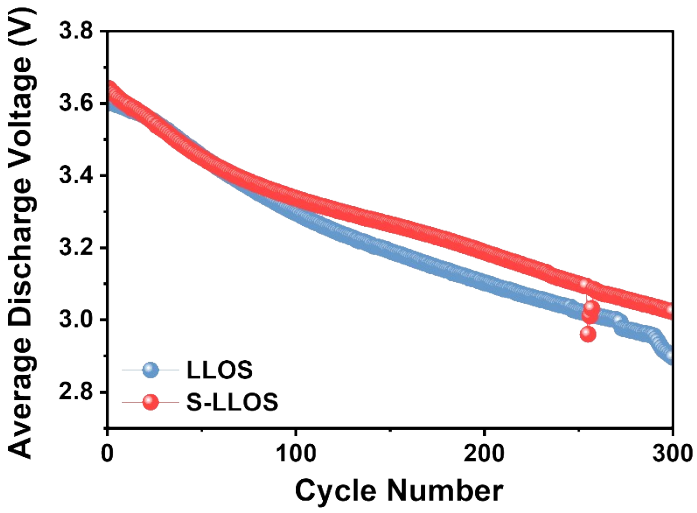

Figure S14.The average discharge voltage of LLOS and S-LLOS at 0 ℃.

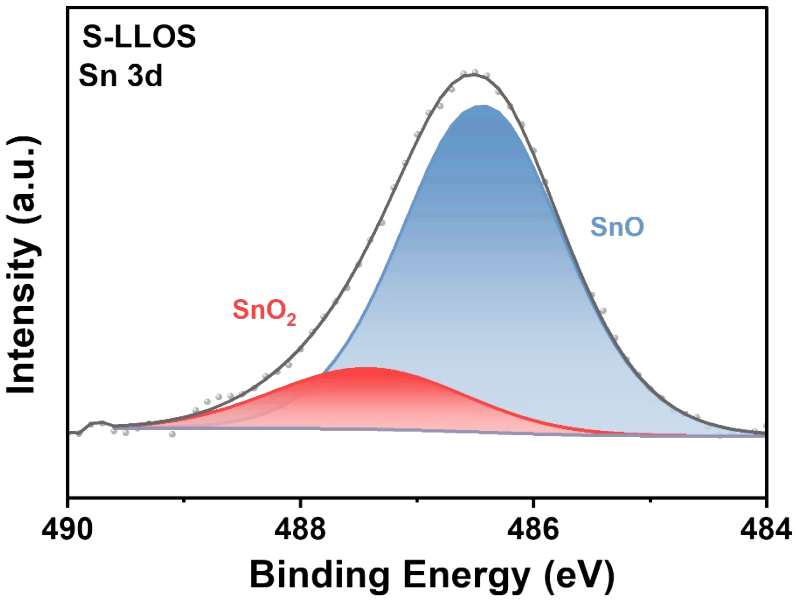

Figure S15. XPS spectrum of Sn 3d for LLOS and S-LLOS samples after five cycles at -20 ℃.

Table S1. XRD refined results of LLOS and S-LLOS.

Refined parameters		Sample	
		LLOS	S-LLOS
$R\bar{3}m$ α=β=γ=90°	a, b (Å)	2.84782	2.84845
	c (Å)	14.21336	14.2137
	V (Å^3)	99.828	99.875
C2/m α=γ=90°	a (Å)	4.93959	4.93521
	b (Å)	8.53278	8.54171
	c (Å)	5.02318	5.01611
	β (°)	109.36	109.171
	V (Å^3)	199.748	199.728
p42/mnm α=β=γ=90°	a	/	4.74124
	c		3.17884
	V (Å^3)		71.458

Table S2. The values derived from the impedance curve fitting.

□	283.15 K		273.15 K		263.15 K		253.15 K	
	R_{CEI}	Rct	R_{CEI}	Rct	R_{CEI}	Rct	R_{CEI}	Rct
LLOS	62.36 Ω	110.3 Ω	88.4 Ω	200.1 Ω	125.6 Ω	508.4 Ω	177.7 Ω	1387 Ω
S-LLOS	17.14 Ω	50.2 Ω	21.3 Ω	95.9 Ω	26.3 Ω	218.4 Ω	34.6 Ω	602.7 Ω

Modifying method	Cutoff voltage	Current density (mA g^{-1})	Cycle number and capacity retention	Ref.
Sulfur-assisted surface modification	2.0-4.8 V	100	200/94.1%	[1]
Fluoride coating and functional doping	2.0-4.8 V	40	120/90.1%	[2]
Higher intralayer configuration entropy	2.1-4.8 V	25	100/93%	[3]
$LiTaO_3$ coating	2.0-4.8 V	25	200/80.3%	[4]
Na doped	2.0-4.8 V	100	200/93.1%	[5]
F-doped and Li_2SnO_3 coating	2.0-4.8 V	25	200/73%	[6]
$LiMn_{1.4}Ni_{0.5}Mo_{0.1}O_4$ Coating and Mo Doped	2.0-4.8 V	25	200/66.8%	[7]
This work	2.0-4.8 V	100	200/97.1%	

Table S3. Room-temperature performance comparison of LLOS cathodes.

Table S4. Low-temperature performance comparison of LLOS cathodes.

Cathode materials	Temperature (°C)	Capacity after modification (mAh g^{-1})	Cycle number and capacity retention	Ref.
$Li_{1.2}Ni_{0.2}Mn_{0.6}O_2$@ Li_2O-B_2O_3	-20 °C	137.1@25 mA g^{-1}	/	[8]
$Li_{1.2}Ni_{0.13}Co_{0.13}Mn_{0.54}O_2$ @AlF_3	-20 °C	109.3@25 mA g^{-1}	/	[9]
LiF decoration on $Li_{1.2}Ni_{0.13}Co_{0.13}Mn_{0.54}O_2$	-20 °C	135@25 mA g^{-1}	10 (100%)	[10]
Li_2TiO_3@Zr-doped-$Li_{1.2}Ni_{0.2}Mn_{0.6}O_2$	-20 °C	130@25 mA g^{-1}	70 (around 94%)	[11]
$Li_{1.2}Ni_{0.13}Co_{0.13}Mn_{0.54}O_2$ @$Li_7La_3Zr_2O_{12}$	-20 °C	134.1@25 mA g^{-1}	/	[12]
This work	-20 °C	109.9@25 mA g^{-1}	200 (95%) 400 (84.2%)	

References

1. Z. Xu, X. Guo, W. Song, J. Wang, T. Qin, Y. Yuan and J. Lu, *Adv Mater*, 2024, **36**, e2303612.

2. H. Zhao, W. Li, J. Li, H. Xu, C. Zhang, J. Li, C. Han, Z. Li, M. Chu and X. Qiu, *Nano Energy*, 2022, **92**.

3. J. Song, F. Ning, Y. Zuo, A. Li, H. Wang, K. Zhang, T. Yang, Y. Yang, C. Gao, W. Xiao, Z. Jiang, T. Chen, G. Feng and D. Xia, *Adv Mater*, 2023, **35**, e2208726.

4. M. Si, D. Wang, R. Zhao, D. Pan, C. Zhang, C. Yu, X. Lu, H. Zhao and Y. Bai, *Adv Sci*, 2020, **7**, 1902538.

5. W. He, P. Liu, B. Qu, Z. Zheng, H. Zheng, P. Deng, P. Li, S. Li, H. Huang, L. Wang, Q. Xie and D. L. Peng, *Advanced Science*, 2019, **6**.

6. D. Wang, T. Xu, Y. Li, D. Pan, X. Lu, Y.-S. Hu, S. Dai and Y. Bai, *ACS Applied Materials & Interfaces*, 2018, **10**, 41802-41813.

7. X. Ji, Y. Xu, H. Feng, P. Wang, Y. Zhou, J. Song, Q. Xia and Q. Tan, *ACS Applied Materials & Interfaces*, 2021, **13**, 47659-47670.

8. S. Chen, L. Chen, Y. Li, Y. Su, Y. Lu, L. Bao, J. Wang, M. Wang and F. Wu, *ACS Appl Mater Interfaces*, 2017, **9**, 8641-8648.

9. B. Zhao, J. Xie, H. Zhuang, X. Liu, W. Li, X. Hu, Y. Jiang and J. Zhang, *Solid State Ionics*, 2020, **347**, 115245.

10. X. Ding, Y.-X. Li, F. Chen, X.-D. He, A. Yasmin, Q. Hu, Z.-Y. Wen and C.-H. Chen, *Journal of Materials Chemistry A*, 2019, **7**, 11513-11519.

11.Yanwu Zhai, Jicheng Zhang, Heng Zhang, Xinzhi Liu, Chin-Wei Wang, Limei Sun, and Xiangfeng Liu, *Journal of The Electrochemical Society*, 2019,**166**, A1323-A1329.

12. C. Shen, Y. Liu, W. Li, X. Liu, J. Xie, J. Jiang, Y. Jiang, B. Zhao and J. Zhang, *J Colloid Interface Sci*, 2022, **615**, 1-9.